2006

Constraints on the Nucleon Strange Form Factors at Q2 ~ 0.1 GeV2

K. A. Aniol

D. S. Armstrong

T. Averett

H. Benaoum

P. Y. Bertin

See next page for additional authors

Original Publication Citation

Aniol, K. A., Armstrong, D. S., Averett, T., Benaoum, H., Bertin, P. Y., Burtin, E., . . . Zheng, X. (2006). Constraints on the nucleon strange form factors at Q^2 ~ 0.1 GeV^2. *Physics Letters B, 635*(5–6), 275-279. doi:http://dx.doi.org/10.1016/j.physletb.2006.03.011

Available online at www.sciencedirect.com
SCIENCE DIRECT®
Physics Letters B 635 (2006) 275–279
PHYSICS LETTERS B
www.elsevier.com/locate/physletb

Constraints on the nucleon strange form factors at $Q^2 \sim 0.1$ GeV^2

HAPPEX Collaboration

K.A. Aniol [a], D.S. Armstrong [b], T. Averett [b], H. Benaoum [c], P.Y. Bertin [d], E. Burtin [e], J. Cahoon [f], G.D. Cates [g], C.C. Chang [h], Y.-C. Chao [i], J.P. Chen [i], Seonho Choi [j], E. Chudakov [i], B. Craver [g], F. Cusanno [k], P. Decowski [l], D. Deepa [m], C. Ferdi [d], R.J. Feuerbach [i], J.M. Finn [b], S. Frullani [k], K. Fuoti [f], F. Garibaldi [k], R. Gilman [n,i], A. Glamazdin [o], V. Gorbenko [o], J.M. Grames [i], J. Hansknecht [i], D.W. Higinbotham [i], R. Holmes [c], T. Holmstrom [b], T.B. Humensky [p], H. Ibrahim [m], C.W. de Jager [i], X. Jiang [n], L.J. Kaufman [f], A. Kelleher [b], A. Kolarkar [q], S. Kowalski [r], K.S. Kumar [f], D. Lambert [l], P. LaViolette [f], J. LeRose [i], D. Lhuillier [e], N. Liyanage [g], D.J. Margaziotis [a], M. Mazouz [s], K. McCormick [n], D.G. Meekins [i], Z.-E. Meziani [j], R. Michaels [i], B. Moffit [b], P. Monaghan [r], C. Munoz-Camacho [e], S. Nanda [i], V. Nelyubin [g,t], D. Neyret [e], K.D. Paschke [f,*], M. Poelker [i], R. Pomatsalyuk [o], Y. Qiang [r], B. Reitz [i], J. Roche [i], A. Saha [i], J. Singh [g], R. Snyder [g], P.A. Souder [c], M. Stutzman [i], R. Subedi [u], R. Suleiman [r], V. Sulkosky [b], W.A. Tobias [g], G.M. Urciuoli [k], A. Vacheret [e], E. Voutier [s], K. Wang [g], R. Wilson [v], B. Wojtsekhowski [i], X. Zheng [w]

[a] *California State University, Los Angeles, Los Angeles, CA 90032, USA*
[b] *College of William and Mary, Williamsburg, VA 23187, USA*
[c] *Syracuse University, Syracuse, NY 13244, USA*
[d] *Université Blaise Pascal/CNRS-IN2P3, F-63177 Aubière, France*
[e] *CEA Saclay, DAPNIA/SPhN, F-91191 Gif-sur-Yvette, France*
[f] *University of Massachusetts Amherst, Amherst, MA 01003, USA*
[g] *University of Virginia, Charlottesville, VA 22904, USA*
[h] *University of Maryland, College Park, MD 20742, USA*
[i] *Thomas Jefferson National Accelerator Facility, Newport News, VA 23606, USA*
[j] *Temple University, Philadelphia, PA 19122, USA*
[k] *INFN, Sezione Sanità, I-00161 Roma, Italy*
[l] *Smith College, Northampton, MA 01063, USA*
[m] *Old Dominion University, Norfolk, VA 23508, USA*
[n] *Rutgers, The State University of New Jersey, Piscataway, NJ 08855, USA*
[o] *Kharkov Institute of Physics and Technology, Kharkov 310108, Ukraine*
[p] *University of Chicago, Chicago, IL 60637, USA*
[q] *University of Kentucky, Lexington, KY 40506, USA*
[r] *Massachusetts Institute of Technology, Cambridge, MA 02139, USA*
[s] *Laboratoire de Physique Subatomique et de Cosmologie, F-38026 Grenoble, France*
[t] *St. Petersburg Nuclear Physics Institute of Russian Academy of Sciences, Gatchina 188350, Russia*
[u] *Kent State University, Kent, OH 44242, USA*
[v] *Harvard University, Cambridge, MA 02138, USA*
[w] *Argonne National Laboratory, Argonne, IL 60439, USA*

Received 4 January 2006; received in revised form 28 February 2006; accepted 6 March 2006

Available online 20 March 2006

Editor: D.F. Geesaman

* Corresponding author.
E-mail address: paschke@jlab.org (K.D. Paschke).

doi:10.1016/j.physletb.2006.03.011

Abstract

We report the most precise measurement to date of a parity-violating asymmetry in elastic electron–proton scattering. The measurement was carried out with a beam energy of 3.03 GeV and a scattering angle $\langle\theta_{\rm lab}\rangle = 6.0^\circ$, with the result $A_{\rm PV} = (-1.14 \pm 0.24({\rm stat}) \pm 0.06({\rm syst})) \times 10^{-6}$. From this we extract, at $Q^2 = 0.099$ GeV^2, the strange form factor combination $G_E^s + 0.080 G_M^s = 0.030 \pm 0.025({\rm stat}) \pm 0.006({\rm syst}) \pm 0.012({\rm FF})$ where the first two errors are experimental and the last error is due to the uncertainty in the neutron electromagnetic form factor. This result significantly improves current knowledge of G_E^s and G_M^s at $Q^2 \sim 0.1$ GeV^2. A consistent picture emerges when several measurements at about the same Q^2 value are combined: G_E^s is consistent with zero while positive values are favored for G_M^s, though $G_E^s = G_M^s = 0$ is compatible with the data at 95% C.L.

PACS: 13.60.Fz; 11.30.Er; 13.40.Gp; 14.20.Dh

1. Introduction

The nucleon is a bound state of three valence quarks, but a rich structure is evident when it is probed over a wide range of length scales in scattering experiments. A "sea" of virtual quark–antiquark pairs of the three light (up, down and strange) flavors and gluons surrounds each valence quark. One way to probe the sea is to investigate whether strange quarks contribute to the static properties of the nucleon. Establishing a non-trivial role for the sea would provide new insight into non-perturbative dynamics of the strong interactions.

In one class of measurements, elastic lepton–nucleon electromagnetic scattering is used to measure electric and magnetic form factors, which are functions of the 4-momentum transfer Q^2 and carry information on the nucleon charge and magnetization distributions. Weak neutral current (WNC) elastic scattering, mediated by the Z^0 boson, measures form factors that are sensitive to a different linear combination of the three light quark distributions. When combined with proton and neutron electromagnetic form factor data and assuming charge symmetry, the strange electric and magnetic form factors G_E^s and G_M^s can be isolated, thus accessing the nucleon's strange quark charge and magnetization distributions [1].

Parity-violating electron scattering is a particularly clean experimental technique to extract the WNC amplitude [2,3]. Such experiments involve the scattering of longitudinally polarized electrons from unpolarized targets, allowing the determination of a parity-violating asymmetry $A_{\rm PV} \equiv (\sigma_R - \sigma_L)/(\sigma_R + \sigma_L)$, where $\sigma_{R(L)}$ is the cross section for incident right (left)-handed electrons. $A_{\rm PV}$ arises from the interference of the weak and electromagnetic amplitudes [4]. Typical asymmetries are small, ranging from 0.1 to 100 parts per million (ppm).

Four collaborations have published $A_{\rm PV}$ measurements in elastic electron–proton scattering. The SAMPLE result [5] at a backward angle constrained G_M^s at $Q^2 \sim 0.1$ GeV^2. The HAPPEX [6], A4 [7,8], and G0 [9] results at forward angles constrained a linear combination of G_E^s and G_M^s in the range $0.1 < Q^2 < 1$ GeV^2. While no measurement independently indicates a significant strange form factor contribution, the A4 measurement at $Q^2 = 0.108$ GeV^2 and the G0 measurement at slightly higher Q^2 each suggest a positive deviation, at the level of $\sim 2\sigma$, from the asymmetry which would be expected with no strange quark contribution [8,9].

In this Letter, we report a new measurement of $A_{\rm PV}$ in elastic electron–proton scattering at $Q^2 \sim 0.1$ GeV^2. This first result from experiment E99-115 at the Thomas Jefferson National Accelerator Facility (JLab) has achieved the best precision on $A_{\rm PV}$ in electron–nucleon scattering. The sensitivity of the measurement to strange form factors is similar to that of the recently published A4 measurement [8]. However, the measurement we describe below employs an analog integrating technique which allows very high instantaneous rates. This will ultimately result in a significant reduction in overall statistical and systematic uncertainties. The goal of the experiment is to reach a precision $\delta(A_{\rm PV}) \sim 0.1$ ppm.

2. Description of the apparatus

The experiment is situated in Hall A at JLab. A 35 μA continuous-wave beam of longitudinally polarized 3.03 GeV electrons is incident on a 20 cm long liquid hydrogen target. The highly polarized (75–85%) electron beam is generated from a strained-layer GaAs photocathode using circularly polarized laser light. Scattered electrons are focused by twin spectrometers onto total-absorption detectors situated in heavily-shielded detector huts, creating a clean separation between elastically scattered electrons and inelastic backgrounds. The spectrometers are arranged to create an approximately left–right symmetric acceptance. This not only doubles the accepted scattered flux as compared to the use of a single spectrometer but also reduces the sensitivity of the total accepted rate to the precise beam trajectory at the target. Each spectrometer accepts approximately 5 mrad of solid angle containing a range in scattering angle of approximately 4°–8°.

Elastically-scattered electrons are focused onto detectors, spatially well-separated from inelastic trajectories by a 12 meter dispersion in the spectrometer optics. The electrons are detected by total absorption calorimeters composed of alternating layers of brass and quartz, oriented such that the Cherenkov light generated by the electromagnetic shower is transported by the quartz to one end of the detector. Two separate detector segments in each spectrometer arm cover the full flux of elastically scattered electrons, for a total of 4 detector photomultiplier tubes (PMTs). The PMT responses are integrated; the detector elements and the associated electronics are designed to accept an elastic flux rate of ~ 100 MHz at full design luminosity.

The experimental configuration is similar to the previous measurement of A_{PV} at $Q^2 \sim 0.5$ GeV^2 [6]. The presently reported measurement is enabled by the addition of septum magnets to accept very-forward scattered electrons with $\langle\theta_{lab}\rangle \sim 6°$, and the introduction of radiation-hard focal plane detectors which can survive the increased scattered electron rate. This configuration is described in more detail in the recent report on the A_{PV} result with a ^{4}He target [10].

The helicity of the polarized electron beam is set every 33.3 ms; each of these periods of constant helicity will be referred to as a "window". The helicity sequence is structured as pairs of windows with opposite helicity ("window pairs"), with the helicity of the first window selected pseudo-randomly. The integrated response of the detector PMTs, beam current monitors, and beam position monitors is digitized and recorded into the data stream for each window.

3. Data sample and analysis

The data sample consists of roughly 11 million helicity-window pairs. Loose requirements are imposed on beam quality which remove periods of current, position, or energy instability from the final data set. However, no helicity-dependent cuts are applied. After applying selection criteria, 9.96×10^6 window pairs remain for further analysis.

The helicity-correlated asymmetry in the integrated detector response, normalized to the average beam current for each window, is computed for each window pair and then corrected for fluctuations in the beam trajectory to form the raw asymmetry A_{raw}. The first order dependence on five correlated beam parameters (energy and horizontal and vertical position and angle) is removed by two independent analysis methods. The first method applies linear regression to the window pairs used in the physics analysis. The second method uses a periodic modulation of beam parameters, performed at regular intervals for this purpose, to calibrate the sensitivity of the accepted rate to changes in the beam trajectory. The numerical difference between the two results is negligible compared to the final statistical uncertainty; results from the second method are quoted in this Letter.

The A_{raw} window-pair distribution has an RMS width of ~ 620 ppm. Non-Gaussian tails are negligible over more than 4 orders of magnitude. This demonstrates that the distribution is dominated by the counting statistics of an elastically scattered electron rate of ~ 40 MHz. Contributions to the fluctuations from background, electron beam, electronic noise or target density are negligible.

The cumulative correction for A_{raw} due to helicity-correlated differences in electron beam position and energy is -0.079 ± 0.032 ppm. This correction is small compared to the statistical error on A_{raw} due to several important factors. First, careful attention is given to the design and configuration of the laser optics in the polarized source to reduce helicity-correlated beam asymmetries to a manageable level. Over the duration of data collection, the cumulative helicity-correlated asymmetries in the electron beam are 0.022 ppm in energy, 8 nm in position, and 4 nrad in angle.

The largest correction of -0.130 ppm is from the beam monitor that is predominantly sensitive to the helicity-correlated beam energy asymmetry. The systematic error in the correction is estimated by studying residual correlations of beam asymmetries with the responses of individual PMTs, in which sensitivity to the beam trajectory is enhanced by the division of the elastic peak over the detector segmentation. Compared to the individual detector segments, the sensitivities to various beam parameters are reduced by factors of 5–20 when averaged over the detector segments and over the left–right symmetric spectrometer arms.

The beam intensity asymmetry, integrated over the run and measured in two independent beam charge monitors, is -2.6 ppm. The average values measured by the two monitors are consistent within the electronic noise limit, estimated to be 0.03 ppm over the full data set. Dedicated calibration runs are used to place upper-limits on the relative non-linearity between the beam monitors and the detectors ($< 0.2\%$) and the absolute non-linearity of the detector PMTs ($< 1\%$), leading to a contribution to systematic uncertainty of 0.015 ppm.

A half-wave ($\lambda/2$) plate is periodically inserted into the laser optical path, passively reversing the sign of the electron beam polarization. Roughly equal statistics are thereby accumulated with opposite signs for the measured asymmetry, which suppresses many systematic effects. Fig. 1 shows A_{raw} for all data, averaged over the 2 PMT channels in each spectrometer, grouped by $\lambda/2$-plate state and divided into 6 sequential samples. The observed fluctuations are consistent with purely statistical fluctuations around the average parity-violating asymmetry, shown on the plot with the expected sign flip due to half wave plate state, with a χ^2 per degree of freedom of 1.0.

The physics asymmetry A_{PV} is formed from A_{raw} by correcting for beam polarization, backgrounds, and finite acceptance:

$$A_{PV} = \frac{K}{P_b} \frac{A_{raw} - P_b \sum_i A_i f_i}{1 - \sum_i f_i}, \tag{1}$$

where P_b is the beam polarization, f_i are background fractions and A_i the associated background asymmetries, and K accounts for the range of kinematic acceptance.

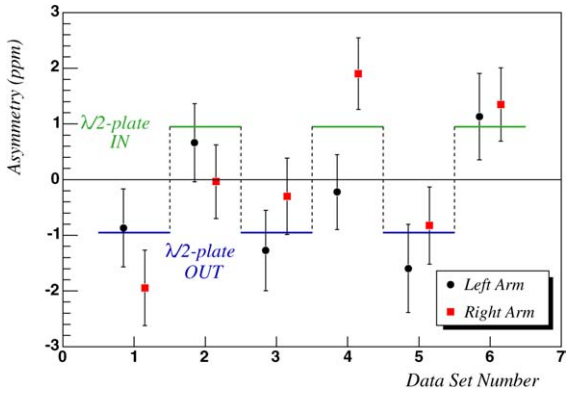

Fig. 1. A_{raw} for all data, grouped by $\lambda/2$-plate state in 6 sequential data sets. The circles and squares represent the average of the 2 PMT channels in each spectrometer arm, and the line represents A_{raw}, averaged over the run and plotted with the appropriate sign for each half-wave plate state.

Table 1
Corrections to $A_{\rm raw}$ and systematic uncertainties

Correction (ppm)	
Target windows	0.006 ± 0.016
Rescatter	0.000 ± 0.031
Beam asyms.	-0.079 ± 0.032
Non-linearity	0.000 ± 0.015
Normalization factors	
Polarization P_b	0.813 ± 0.016
Acceptance K	0.976 ± 0.006
Q^2 scale	1.000 ± 0.015

The beam polarization measured by the Hall A Compton polarimeter [11] is determined to be $P_b = 0.813 \pm 0.016$, averaged over the duration of the run. The result is consistent, within systematic uncertainties, with dedicated polarization measurements using Møller scattering in Hall A and Mott scattering in the low-energy injector.

Drift chambers are used to track individual events at the spectrometer focal plane during dedicated, low-current runs in order to determine the average kinematics and to study backgrounds to the integrating measurement. The average Q^2 is determined to be $\langle Q^2 \rangle = 0.099 \pm 0.001$ GeV^2; the uncertainty in this value contributes to the systematic error of the asymmetry. The acceptance correction to account for the non-linear dependence of the asymmetry with Q^2 is computed, using a Monte Carlo simulation, to be $K = 0.976 \pm 0.006$.

Largely due to the excellent hardware resolution of the spectrometers ($\delta p/p < 0.1\%$), the total dilution of the PMT response from all background sources is less than 1%. The largest contribution of 0.9% comes from the aluminum windows of the cryogenic target. The asymmetry of this background is assumed to be that of quasi-elastic scattering from aluminum, calculated as described in [12]. A relative uncertainty of 50% is assigned to this calculated asymmetry. The asymmetry of this background is of the same sign and similar magnitude to that of $A_{\rm PV}$ from elastic scattering off hydrogen, which reduces its total contribution to the systematic uncertainty of this measurement.

While only elastically scattered electrons directly reach the detectors from the target, dedicated runs are used to estimate the contribution from charged particles which rescatter inside the spectrometers. Rates in the detectors are studied as the central spectrometer momentum is varied. Individual scattered electrons are tracked to determine the locations of rescattering in the spectrometer. From these studies, an upper limit on $A_{\rm PV}$ due to possible rescattering from polarized iron or unpolarized material is determined to be 0.031 ppm.

The corrections are summarized in Table 1. After all corrections, the result at $Q^2 = 0.099$ GeV^2 is

$$A_{\rm PV} = -1.14 \pm 0.24(\text{stat}) \pm 0.06(\text{syst}) \text{ ppm}. \tag{2}$$

4. Results and conclusions

The parity-violating asymmetry is given in the standard model by [3]:

$$\begin{aligned} A_{\rm PV} = -\frac{G_F Q^2}{4\pi\alpha\sqrt{2}} \times \Big\{ & \big(1 + R_V^p\big)\big(1 - 4\sin^2\theta_W\big) \\ & - \big(1 + R_V^n\big)\frac{\epsilon G_E^{\gamma p} G_E^{\gamma n} + \tau G_M^{\gamma p} G_M^{\gamma n}}{\epsilon (G_E^{\gamma p})^2 + \tau (G_M^{\gamma p})^2} \\ & - \big(1 - R_V^{(0)}\big)\frac{\epsilon G_E^{\gamma p} G_E^{s} + \tau G_M^{\gamma p} G_M^{s}}{\epsilon (G_E^{\gamma p})^2 + \tau (G_M^{\gamma p})^2} \\ & - \frac{(1 - 4\sin^2\theta_W)\,\epsilon' G_M^{\gamma p}}{\epsilon (G_E^{\gamma p})^2 + \tau (G_M^{\gamma p})^2}\big[-2\big(1 + R_A^{T=1}\big)G_A^{T=1} \\ & + \big(\sqrt{3} R_A^{T=0}\big) G_A^{T=0}\big] \Big\} \end{aligned} \tag{3}$$

with

$$\tau = \frac{Q^2}{4M_P^2}, \qquad \epsilon = \left[1 + 2(1+\tau)\tan^2\left(\frac{\theta}{2}\right)\right], \quad \text{and}$$

$$\epsilon' = \sqrt{\tau(1+\tau)\big(1-\epsilon^2\big)}.$$

$G_{E(M)}^{\gamma p(n)}$ are the proton (neutron) electric (magnetic) form-factors, $G_A^{T=1(0)}$ is the isovector (isoscalar) proton axial form factor, G_F is the Fermi constant, α is the fine structure constant, and θ_W is the electroweak mixing angle. All form factors are functions of Q^2. The $R_{V,A}$ factors parametrize the electroweak radiative corrections of the neutral weak current [3]. All the vector corrections [3] and the axial corrections [13] are calculated using the ($\overline{\rm MS}$) renormalization scheme; in this scheme $\sin^2\theta_W \equiv \sin^2\hat{\theta}_W(M_Z) = 0.23120(15)$ [14]. Corrections due to purely electromagnetic radiative corrections are negligible due to the small momentum acceptance ($\delta p/p < 3\%$) and the spin independence of soft photon emission [15].

At the central kinematics $\epsilon = 0.994$, $\tau = 0.028$, and $\epsilon' = 0.018$. The values for the electromagnetic form factors $G_{E(M)}^{\gamma p(n)}$ are taken from a recently published phenomenological fit to world data at low Q^2 [16], with uncertainties in each value based on error bars of data near $Q^2 = 0.1$ GeV^2. The values (and relative uncertainty) used are: $G_E^p = 0.754$ (2.5%), $G_M^p = 2.144$ (1.5%), $G_E^n = 0.035$ (30.0%), and $G_M^n = -1.447$ (1.5%). The contribution from axial form factors [17,18] is calculated, assuming a dipole form, to be -0.026 ± 0.008 ppm at these kinematics. Sensitivity to possible strange quark contributions to the axial form factor is neglected.

The theoretical value for the asymmetry is calculated at the central kinematics from Eq. (3), using the inputs detailed above and the assumption that strange quarks do not contribute ($G^s = 0$), to be $A_{\rm PV}^{(s=0)} = -1.43 \pm 0.11(\text{FF})$ ppm where the error comes mainly from the uncertainty in G_E^n. Comparing $A_{\rm PV}^{(s=0)}$ to our measured $A_{\rm PV}$ we extract the value of the linear combination of strange form-factors to which this measurement is sensitive: $G_E^s + 0.080 G_M^s = 0.030 \pm 0.025(\text{stat}) \pm 0.006(\text{syst}) \pm 0.012(\text{FF})$ at $Q^2 = 0.099$ GeV^2.

This result is displayed in Fig. 2, along with three other published strange form factor measurements. Each of these measurements was carried out in a narrow Q^2 range of 0.09–0.11 GeV^2 such that combining them introduces no significant additional uncertainty. From the four measurements

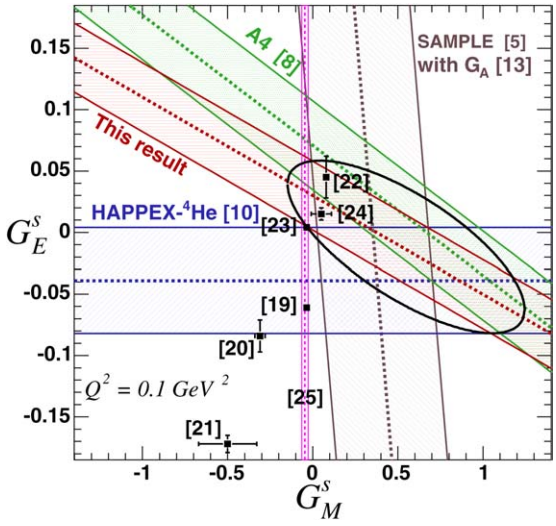

Fig. 2. The four A_{PV} measurements at $Q^2 = 0.09$–0.11 GeV^2 are shown, with shaded bands representing the 1-sigma combined statistical and systematic uncertainties. Also shown is the combined 95% C.L. ellipse from all four measurements. The black squares and narrow vertical band represent various theoretical calculations [19–25].

shown in the figure, limits on G_E^s and G_M^s at $Q^2 \sim 0.1$ GeV^2 are extracted without any additional assumptions. The absence of theoretical guidance for the Q^2 dependence of the form factors precludes the use of published data from higher Q^2 for this fit. The 95% allowed contour from the combined fit is shown in Fig. 2. The best fit values are $G_E^s = -0.01 \pm 0.03$ and $G_M^s = +0.55 \pm 0.28$. While this fit favors positive values for G_M^s, the origin ($G^s = 0$) is still allowed at the 95% C.L. Fig. 2 also shows results from various theoretical calculations [19–25].

In conclusion, we report a precise measurement of A_{PV} in elastic electron–proton scattering at $Q^2 = 0.099$ GeV^2 which has resulted in improved constraints on the strange form factors at $Q^2 \sim 0.1$ GeV^2. The HAPPEX measurements at $Q^2 \sim 0.1$ GeV^2 from both ^{1}H and ^{4}He targets will be improved by a factor of 2 to 3 in precision by additional data collected in late 2005. Given the currently allowed region in Fig. 2, such precision has the potential to dramatically impact our understanding of the role of strange quarks in the nucleon.

Acknowledgements

We wish to thank the entire staff of JLab for their efforts to develop and maintain the polarized beam and the experimental apparatus. This work was supported by DOE contract DE-AC05-84ER40150 Modification No. M175, under which the Southeastern Universities Research Association (SURA) operates JLab, and by the Department of Energy, the National Science Foundation, the INFN (Italy), and the Commissariat à l'Énergie Atomique (France).

References

[1] D.B. Kaplan, A. Manohar, Nucl. Phys. B 310 (1988) 527.
[2] R.D. McKeown, Phys. Lett. B 219 (1989) 140.
[3] M.J. Musolf, et al., Phys. Rep. 239 (1994) 1.
[4] Ya.B. Zel'dovich, Sov. Phys. JETP 36 (1959) 964.
[5] D.T. Spayde, et al., Phys. Lett. B 583 (2004) 79.
[6] K.A. Aniol, et al., Phys. Lett. B 509 (2001) 211;
K.A. Aniol, et al., Phys. Rev. C 69 (2004) 065501.
[7] F.E. Maas, et al., Phys. Rev. Lett. 93 (2004) 022002.
[8] F.E. Maas, et al., Phys. Rev. Lett. 94 (2005) 152001.
[9] D.S. Armstrong, et al., Phys. Rev. Lett. 95 (2005) 092001.
[10] K.A. Aniol, et al., Phys. Rev. Lett. 96 (2006) 022003.
[11] S. Escoffier, et al., Nucl. Instrum. Methods A 551 (2005) 563.
[12] M.J. Musolf, T.W. Donnelly, Nucl. Phys. A 546 (1992) 509.
[13] S.-L. Zhu, et al., Phys. Rev. D 62 (2000) 033008.
[14] J. Erler, P. Langacker, Phys. Lett. B 592 (2004) 114.
[15] L.C. Maximon, W.C. Parke, Phys. Rev. C 61 (2000) 045502.
[16] J. Friedrich, Th. Walcher, Eur. Phys. J. A 17 (2003) 607.
[17] Y. Goto, et al., Phys. Rev. D 62 (2000) 034017.
[18] A. Bodek, H. Budd, J. Arrington, AIP Conf. Proc. (USA) 698 (2003) 148.
[19] N.W. Park, H. Weigel, Nucl. Phys. A 451 (1992) 453.
[20] H.W. Hammer, U.G. Meissner, D. Drechsel, Phys. Lett. B 367 (1996) 323.
[21] H.-W. Hammer, M.J. Ramsey-Musolf, Phys. Rev. C 60 (1999) 045204.
[22] A. Silva, et al., Phys. Rev. D 65 (2001) 014015.
[23] V. Lyubovitskij, et al., Phys. Rev. C 66 (2002) 055204.
[24] R. Lewis, et al., Phys. Rev. D 67 (2003) 013003.
[25] D.B. Leinweber, et al., Phys. Rev. Lett. 94 (2005) 212001.